Journal of Orthopaedic Surgery and Research

RESEARCH ARTICLE Open Access

YBX1 alleviates ferroptosis in osteoporosis via the ATF4/FSP1 axis in an m^5C manner

Lei Tong[1], Yanbo Chen[1], Yan Gao[1], Xiaoming Gao[1] and Yanming Hao[1*]

Abstract

Background Interactions between RNA-binding proteins and RNA regulate RNA transcription during osteoporosis. Ferroptosis, a programmed cell death caused by iron metabolism, plays a vital role in osteoporosis. However, the mechanisms by which RNA-binding proteins are involved in ferroptosis during osteoporosis remain unclear.

Methods We established an in vitro model of osteoporosis induced by D-galactose (D-gal) in MC3T3-E1 cells. Ferroptosis suppressor protein 1 (FSP1), activating transcription factor 4 (ATF4), and Y-box binding protein 1 (YBX1) knockdown MC3T3-E1 cells were generated, and their effects on ferroptosis were verified by measuring lipid reactive oxygen species levels and cellular Fe^{2+}. Chromatin immunoprecipitation and luciferase assays were performed to confirm the binding of ATF4 to the FSP1 promoter. RNA pulldown and RNA immunoprecipitation experiments were used to determine the binding between YBX1 and ATF4 mRNA and to test the effect of YBX1 on ATF4 mRNA stability in a 5-methylcytosine (m^5C)-dependent manner.

Results FSP1 or YBX1 knockdown led to a D-gal-induced increase in lipid reactive oxygen species levels and cellular Fe^{2+} in MC3T3-E1 cells, which was alleviated by ATF4 overexpression. ATF4 inhibits ferroptosis by binding to the FSP1 promoter. In addition, YBX1 increased ATF4 mRNA stability through m^5C RNA modification and inhibited ferroptosis in MC3T3-E1 cells via the ATF4/FSP1 axis.

Conclusion Our results showed that YBX1 could alleviate ferroptosis via the ATF4/FSP1 axis in an m^5C-dependent manner in D-gal-induced osteoblasts, suggesting that YBX1 may be a new target for osteoporosis treatment.

Keywords Osteoporosis, Ferroptosis, Y-box binding protein 1, Activating transcription factor 4, Ferroptosis suppressor protein 1

Introduction

Osteoporosis is a systemic bone disease characterized by increased bone fragility, mainly manifested by decreased bone mass and the destruction of bone microarchitecture [1]. Statistically, 40% of women and 30% of men will develop fractures caused by osteoporosis in the future [2]. Estrogens, bisphosphonates, and selective estrogen receptor modulators 2 are widely used clinically to prevent and treat osteoporosis [3–7]. However, these drugs can lead to the development of malignant cardiovascular events, thromboembolism, gastrointestinal symptoms, pain, and other side effects [8]. Therefore, new therapeutic approaches for osteoporosis and the minimization of side effects are urgently needed.

Ferroptosis is a form of cell death regulated primarily by iron metabolism. Recently, key genes and related biomarkers for ferroptosis have been identified in the mesenchymal stromal cells of patients with osteoporosis, which may mediate bone remodeling by regulating

*Correspondence:
Yanming Hao
yanminghaodr1314@126.com
Full list of author information is available at the end of the article

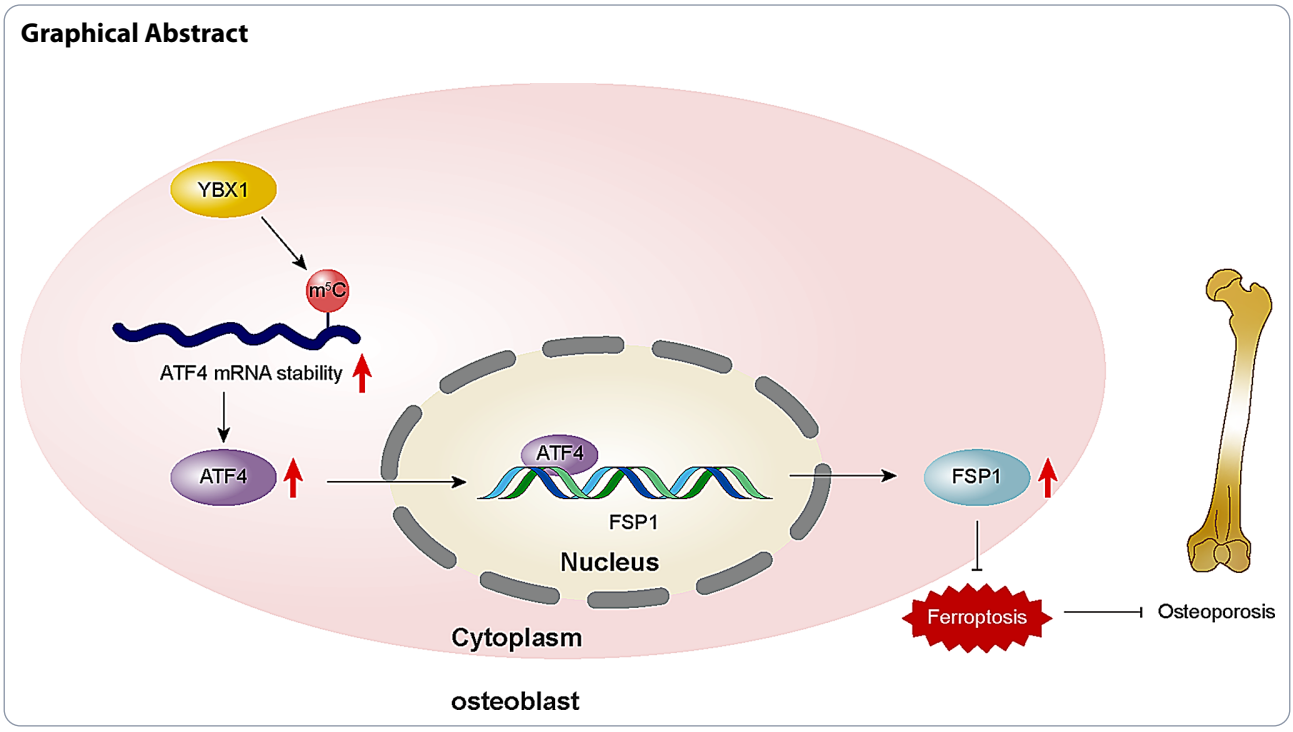

osteoblasts and osteoclasts [9]. Thus, the inhibition of ferroptosis may be a key element in alleviating osteoporosis. Ferroptosis suppressor protein 1 (FSP1), also known as apoptosis-inducing factor mitochondria-associated 2, is an anti-ferroptotic protein [10]. FSP1 may mediate bone tumor development by regulating iron metabolism, reactive oxygen species (ROS) generation, and lipid peroxidation. It also suppresses bone loss by regulating ferroptosis in macrophages [11]. Therefore, promoting FSP1 expression may help improve osteoporosis by preventing ferroptosis.

Activating transcription factor 4 (ATF4) is a basic leucine zipper transcription factor that is found in many tissues [12]. ATF4 can inhibit hepatocellular carcinoma and combat drug-mediated cardiotoxicity by inhibiting ferroptosis. ATF4 promotes osteoclast differentiation and enhances osteoblast activity [13]. It is predicted, based on the JASPAR database (https://jaspar.elixir.no/), that ATF4 binds to the FSP1 promoter [14], indicating that ATF4 might transcriptionally activate FSP1 to mediate the inhibition of ferroptosis in osteoblasts, ultimately ameliorating osteoporosis.

5-methylcytosine (m^5C) is widely found in mRNAs, rRNAs, and tRNAs as a reversible epigenetic modification involved in RNA processing and participates in various biological processes, such as protein binding and RNA stability regulation [15]. During ferroptosis, RNA m^5C modification may limit liver failure and pancreatic cell damage by inhibiting ferroptosis. In previous studies, m^5C modification was found to be extensively involved in the progression of bone disease, exerting a dual regulatory role in osteogenic differentiation [16]. Due to the bioeffects of ATF4 and m^5C modification, we predicted the sequence of the m^5C modification site on ATF4 mRNA based on PACES (http://www.rnanut.net/paces/) (Figure S1A). Further Rm2target analysis (http://rm2target.canceromics.org/#/home) (Figure S1B) showed that Y-box binding protein 1 (YBX1) binds to all the m^5C binding sites on ATF4 mRNA. YBX1 acts as a reader of m^5C and has been shown to promote angiogenesis-dependent osteogenesis and ameliorate bone loss [17].

Collectively, we propose that YBX1 may increase the recognition function of the m^5C site on ATF4 mRNA, which in turn upregulates the expression of ATF4 by increasing the stability of ATF4 mRNA, further promoting the expression of FSP1 and ultimately inhibiting ferroptosis in osteoblasts to alleviate osteoporosis. Our project provides insights for a more comprehensive understanding of the pathological mechanisms of osteoporosis and potential therapeutic targets for subsequent treatment.

Materials and methods

Cell culture

Mouse osteoblast-like (MC3T3-E1) cells (CRL-2593, American Type Culture Collection, Manassas, Virginia, USA) were cultured in alpha-Minimum Essential Medium. As a model cell line, 293T cells exhibit good transfection efficiency and are better suited for mechanism validation and protein interaction experiments [18].

Table 1 The shRNA sequences

Gene	Name	shRNA targeting sequences
FSP1	SH1	5′- GCTAGCAATGGTGCTCTGAAA – 3′
	SH2	5′- CAGGGCAAAGTGATTGGCATA – 3′
	SH3	5′- CAATGAGTATCGGGAGTACAT – 3′
	SH4	5′- CATAGACTTGAAGAACCGGAT – 3′
YBX1	SH1	5′- ACAGAATATGTATCGCCCTTA – 3′
	SH2	5′- GAGAACCCTAAACCACAAGAT – 3′
	SH3	5′- GTATCGCCGAAACTTCAATTA – 3′
	SH4	5′- CATCTCTACCATCATCCGGTT – 3′
ATF4	SH1	5′- GCGAGTGTAAGGAGCTAGAAA – 3′
	SH2	5′- GACCCACCTGGAGTTAGTTTG – 3′
	SH3	5′- TGCTGCTTACATTACTCTAAT – 3′
	SH4	5′- CTAGGTCTCTTAGATGACTAT – 3′

293T cells (CL-0005; Procell Life Science & Technology, Wuhan, China) were cultured in Dulbecco's Modified Eagle's medium. Cells were incubated with 10% fetal bovine serum and penicillin-streptomycin in an incubator containing 5% CO_2 at 37℃. The cells were then cultured in 96-well plates for further treatment. For the establishment of an in vitro osteoporosis model, MC3T3-E1 cells were cultured with D-galactose (D-gal) (25.5 mM) in alpha-Minimum Essential Medium, as previously described [19]. All genetic recombination experiments were approved by Kunshan First People's Hospital.

Cell transfection

Short hairpin RNA (shRNA) targeting FSP1 (shFSP1), ATF4 (shATF4), and YBX1 (shYBX1) (see Table 1 for details), negative control shRNA (shNC), ATF4 overexpression plasmid (ATF4), and negative control plasmid (NC) were obtained from Fenghbio (Changsha, China). MC3T3-E1 cells were seeded in 24-well plates at a density of 2×10^5 cells/well and transfected with 100 nM shRNA for 48 h to knockdown gene expression using 0.75 μL Lipofectamine 3000 (L3000075, Invitrogen, Carlsbad, CA). After incubation, the cells were treated with D-gal, which induced impaired osteogenesis for subsequent analyses.

Cell viability assay

Cell Counting Kit-8 (CCK-8) assay kits (Sigma-Aldrich, St. Louis, MO, USA) were used to determine cell viability with or without the ferroptosis inhibitor ferrostatin-1 (Fer-1) (S7243, Selleck Chemicals, TX, United States) or deferoxamine (DFO) (D0160000, Sigma-Aldrich) in MC3T3-E1 cells, with dimethyl sulfoxide (DMSO) as a negative control. Briefly, MC3T3-E1 cells were plated in 96-well plates at a density of 5×10^3 cells/well for 24 h. Fer-1 (1 mg/mL) or DFO (1 mg/mL) was then added, followed by the addition of 10 μL of CCK-8 solution (5 mg/mL) for 2 h at 37 °C. Optical density at 450 nm was measured using a microplate analyzer.

Table 2 The mutant variants sequence of promoters of FSP1 and ATF4

Name	Variant	Sequences
FSP1-BS1 (-1288/-1279)	wide type	5′- ATGTATCTAAG-3′
	mutant	5′- TACTAGATTC-3′
FSP1-BS2 (-1445/-1436)	wide type	5′- ATGATGGAAA-3′
	mutant	5′- TACTACCTTT-3′
ATF4 (370/384)	wide type	5′- CTTCCCCTCCCGCAG-3′
	mutant	5′- GAAGGGGAGGGCGTC-3′

Western blot

The cells were lysed in RIPA buffer containing phenylmethylsulfonyl fluoride and protease inhibitors. After centrifugation at 12,000 rpm, the supernatant was collected, and protein concentrations were measured using a BCA assay kit (Beyotime, Jiangsu, China). A total of 10 μg of protein was loaded onto a sodium dodecyl sulfate-polyacrylamide gel electrophoresis for electrotransfer, followed by blocking with 5% milk and incubation with primary antibodies. The primary antibodies used were ATF4 (ab85049, Abcam, Cambridge, MA, UK), FSP1 (ab197896, Abcam), YBX1 (ab76149, Abcam), and β-actin (ab8227, Abcam). The following day, the membranes were incubated with secondary antibodies (ab288151, Abcam) and visualized using a chemiluminescent horse radish peroxidase (HRP) substrate (ECL).

RNA pulldown

Specific ATF4 biotinylated probes (5'-CTTTCCTCTTC CCTCCCGCAGGGCTTG-3') and antisense ATF4 biotinylated probes (5'-GAAAGGAGAAGGGAGGGCGTCC CGAAC-3') were purchased from Roche (11685597910). After incubation with the biotin-labeled probe and Streptavidin Magnetic Beads for 4 h at 4℃ (following the manufacturer's instructions), the complexes were pulled down using a magnetic stand. A RNeasy Mini Kit (Qiagen, Hilden, Germany), coupled with magnetic beads, was used to purify and extract RNA. Finally, western blot analysis was performed to detect YBX1 protein in the isolated complex.

Luciferase assay

To explore the effects of ATF4 on FSP1 promoter activity, wild-type (WT) or mutated (Mut) FSP1 promoter sequences (please see Table 2 for the sequences and location), constructed by Cyagen Bioscience (Suzhou, China), were inserted into a psiCHECK-2 vector (Promega, Madison, WI, USA). A total of 2×10^5 293T and MC3T3-E1 cells were transfected with the established luciferase reporter plasmids together with 100 nM shNC or shATF4 using Lipofectamine 3000 transfection reagent (Invitrogen). After incubation for 48 h, the luciferase activity of ATF4 on the FSP1 promoter was measured using a Dual-Luciferase Reporter Assay Kit (Promega).

To explore the influence of YBX1 on the m^5C locus of ATF4 mRNA (Gene ID: 11911; NM_001287180.1), the fragment of ATF4 mRNA, which was acquired from NCBI database (https://www.ncbi.nlm.nih.gov/home/develop/), including the wild-type (ATF4-WT) or mutant (ATF4-Mut) binding sites with m^5C locus (please see Table 2 for the sequences and location), constructed by Cyagen Bioscience (Suzhou, China), were inserted into the psiCHECK-2 vector (Promega). A total of 2×10^5 cells/well of 293T and MC3T3-E1 cells were transfected with the established luciferase reporter plasmids together with ATF4-WT or ATF4-Mut in combination with 100 nM shNC or shYBX1 using Lipofectamine 3000 transfection reagent (Invitrogen). After 48 h of transfection, the luciferase activity of YBX1 on ATF4 mRNA was determined using a dual-luciferase reporter assay kit.

Measurement of lipid ROS and cellular Fe^{2+}

C11-BODIPY 581/591 fluorescent dye (D3861, Life Technologies, Waltham, CA, USA) was used to detect lipid ROS. MC3T3-E1 cells were incubated with 5 μM of C11-BODIPY, followed by incubation for an additional 20 min at 37 °C. MC3T3-E1 cells were then collected by trypsinization, resuspended in 400 μL of PBS, filtered through a 35 μm nylon mesh filter, and subjected to flow cytometry analysis with a 488 nm laser for excitation (BD Biosciences GmbH).

Iron assay kits (ab83366; Abcam) were used to detect cellular Fe^{2+}. Briefly, iron reducer and assay buffer were mixed and incubated with the cells. After incubation with the iron probe, the absorbance was measured using a colorimetric microplate reader (optical density: 593 nm).

RNA stability assay

After shYBX1 transfection for 24 h in the MC3T3-E1 cells, the cells were treated with 5 μg/mL actinomycin D (HY-17559, MedChemExpress, Monmouth Junction, NJ, USA) or DMSO as a control. Subsequently, the remaining RNA was extracted for further RT-qPCR analysis.

RT-qPCR

RNA from the cells was extracted using TRIzol reagent (15596-026, Invitrogen) and reverse-transcribed into cDNA using a reagent kit (Takara Bio, Tokyo, Japan). RT-qPCR was then conducted using SYBR Green Master Mix (Takara Bio, Japan) on a QuantStudio v5 system (Thermo Fisher, Waltham, MA, USA). The comparative threshold cycle ($2^{-\Delta\Delta Ct}$) method was used to analyze the data. The primer sequences are listed in Table 3.

RNA immunoprecipitation (RIP)

The Magna RIP RNA-Binding Protein Immunoprecipitation Kit (17700, Sigma-Aldrich) was used for RIP analysis. MC3T3-E1 cells were lysed with RIP buffer to cross-link protein-RNA complexes. After centrifugation, the cell nuclei were collected and resuspended in RIP buffer for mechanical shearing of the chromatin. YBX1 antibodies (ab76149; Abcam, Cambridge, UK) were added to the supernatant with magnetic beads. After elution, the precipitated ATF4 mRNA was analyzed by quantitative real-time polymerase chain reaction (RT-qPCR) using the primers listed in Table 3.

Table 3 RT-qPCR primers information used in the manuscript

Gene		Sequences
mouse YBX1	forward	5′-GGATGGCAATGAAGAGGACAAA-3′
	reverse	5′- CGTCTGCGTCGGTAATTGAAGT – 3′
mouse ATF4	forward	5′-AAACCTCATGGGTTCTCCAG-3′
	reverse	5′-GGCATGGTTTCCAGGTCATC-3′
mouse β-actin	forward	5′- CTGCTGACGGCCAGGT-3′
	reverse	5′- TGGATGCCACAGGATTCCAT-3′

Table 4 The primer of FSP1 promoters used in ChIP-qPCR

Name		Sequences
FSP1-BS1	forward	5′- ATGGCTGGACCTTGGTGTTC – 3′
	reverse	5′- GAAGCTACCTGAAGGGCTCC – 3′
FSP1-BS2	forward	5′- ACCATGTATGTCGTGCCTGG – 3′
	reverse	5′- CATACATAGGCAGTAGGTAGC – 3′

Promoter prediction

The FSP1 (Gene ID: 20198; NM_001410571.1) promoter, that is, the location of the FSP1 transcription start site at 2000 bp upstream and 100 bp downstream (-2000 bp/100 bp), was obtained from the UCSC Genome Browser (https://genome-asia.ucsc.edu/). Through the JASPAR database (https://jaspar.elixir.no/), the binding sites of ATF4 on the FSP1 promoter region were analyzed. Finally, the potential binding sites (BS1 and BS2) of ATF4 on the FSP1 promoter were predicted, and the BS1 and BS2 primers are listed in Table 4.

Chromatin immunoprecipitation (ChIP)

Following the standard ChIP protocol, MC3T3-E1 cells were fixed with 1% formaldehyde, and the supernatant was collected after centrifugation for immunoprecipitation with an anti-ATF4 antibody (ab85049, Abcam) or an IgG antibody (ab205718, Abcam). After precipitation of endogenous DNA-protein complexes with Sepharose and extraction of DNA fragments, the binding of FSP1 promoter fragments to ATF4 was detected by agarose gel electrophoresis.

Statistical analysis

All data are based on three independent experiments and are presented as mean±standard deviation (SD). SPSS 20.0 was used to analyze statistical significance, which was determined using one-way analysis of variance,

followed by Tukey's post hoc test. $P<0.05$ was considered statistically significant (* $P<0.05$, ** $P<0.01$, and *** $P<0.001$).

Results

FSP1 knockdown in MC3T3-E1 cells induced ferroptosis

Osteoporosis in vitro was established using D-gal (25.5 mM) in MC3T3-E1 cells for 48 h [19]. First, we used the CCK-8 assay to evaluate the effects of the ferroptosis inhibitors Fer-1 and DFO on MC3T3-E1 cells. The results showed that cell viability in the high-glucose (HG) group was significantly decreased, and Fer-1 and DFO prevented this reduction, suggesting that D-gal induced ferroptosis in MC3T3-E1 cells (Fig. 1A). Western blotting results showed that the level of FSP1 was reduced after HG induction in MC3T3-E1 cells but remained unchanged after Fer-1 treatment (Fig. 1B).

Subsequently, we constructed FSP1 knockdown MC3T3-E1 cells, and successful knockdown of FSP1 was validated by western blotting (Fig. 1C). Furthermore, silencing FSP1 exacerbated the HG-induced downregulation of FSP1 expression in MC3T3-E1 cells, indicating that FSP1 knockdown was effective in an in vitro osteoporosis model (Fig. 1D). Ferroptosis is characterized by the accumulation of ROS when iron metabolism is abnormal [20]. Lipid ROS and cellular Fe^{2+} were used as measurement indicators. The results showed that HG elevated the levels of lipid ROS and cellular Fe^{2+}, and this effect was further increased after FSP1 knockdown (Fig. 1E–F), indicating that inhibiting FSP1 promotes ferroptosis.

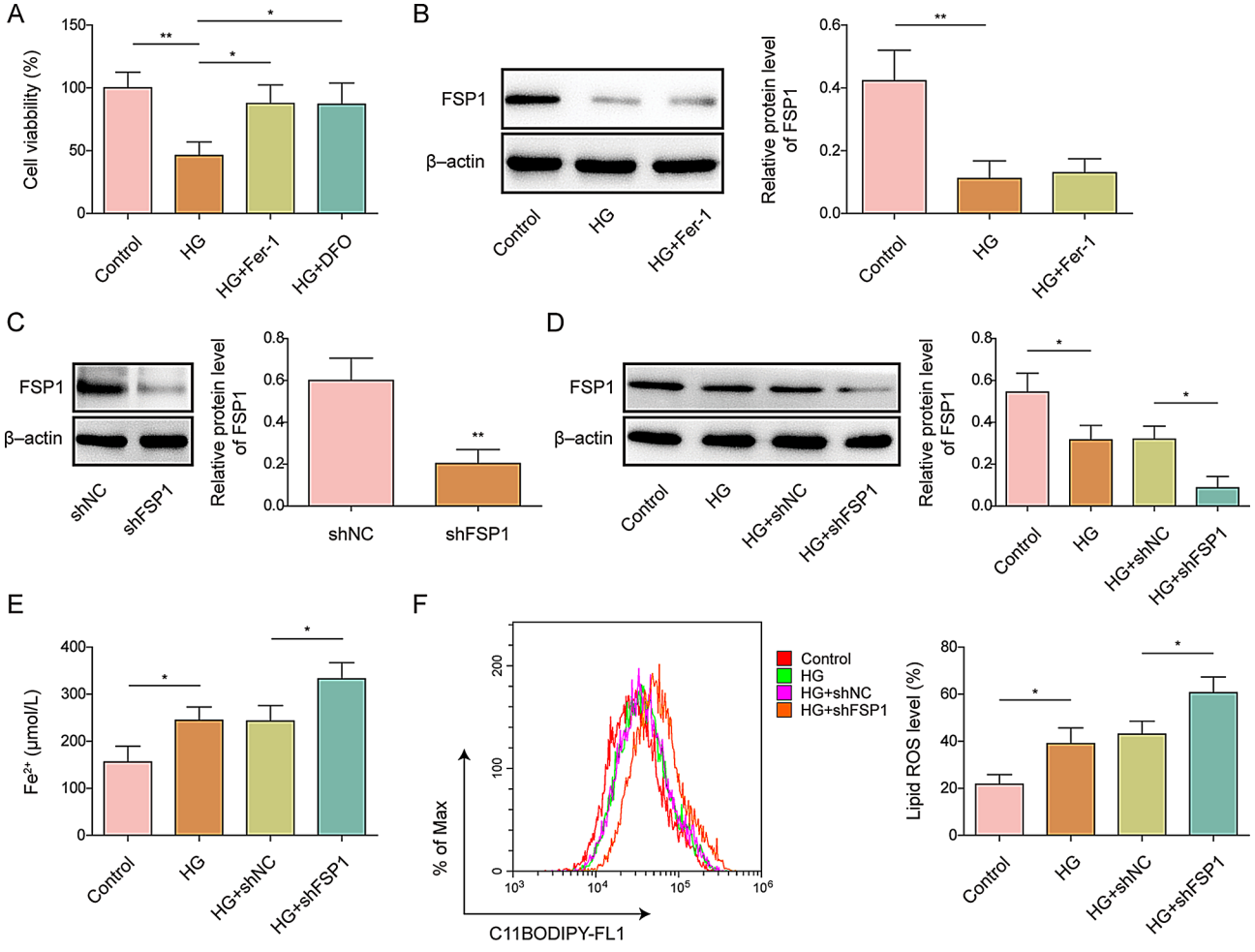

Fig. 1 The effect of FSP1 in MC3T3-E1 cells on ferroptosis MC3T3-E1 cells were used to construct an in vitro osteoporosis model by treating them with D-galactose (25.5 mM) or without (control). Subsequently, the cells were treated with Ferrostatin-1 (Fer-1) or deferoxamine (DFO), and (A) cell viability was assessed (**A**). (**B**) FSP1 protein expression levels in high-glucose (HG)-induced MC3T3-E1 cells, with or without Fer-1 treatment, were measured, and protein quantification was performed. (**C**) FSP1 protein expression levels and quantification after FSP1 knockdown in MC3T3-E1 cells. (**D**) FSP1 protein expression levels in shFSP1- or shNC-transfected HG-exposed MC3T3-E1 cells were evaluated. (**E**) Cellular Fe^{2+} concentrations in shFSP1- and shNC-transfected HG-induced MC3T3-E1 cells were measured. (**F**) Lipid ROS levels in shFSP1- and shNC-transfected HG-exposed MC3T3-E1 cells were evaluated. $n=3$. Data are shown as mean ± SD. * $P<0.05$, ** $P<0.01$, and *** $P<0.001$. FSP1, Ferroptosis suppressor protein 1; ROS, reactive oxygen species

ATF4 bound to the promoter of FSP1 to inhibit ferroptosis in MC3T3-E1 cells

ATF4 is a key transcription factor in bone formation that regulates ferroptosis through different mechanisms [17]. In our study, HG induced a reduction in the expression of ATF4, and this reduction remained unchanged after Fer-1 treatment (Fig. 2A). In addition, using JASPAR database analysis, we found that ATF4 could bind to the FSP1 promoter, and further ChIP assays confirmed that ATF4 might bind to BS1 and BS2 of the FSP1 promoter (Fig. 2B, C). To investigate the effect of ATF4, we constructed ATF4 knockdown MC3T3-E1 cells and found that the expression levels of both ATF4 and FSP1 were significantly reduced (Fig. 2D). Moreover, depletion of ATF4 abrogated the binding of ATF4 to the FSP1 promoter, confirming the effect of ATF4 binding to FSP1 promoter in MC3T3-E1 cells (Fig. 2E). Results from a dual-luciferase reporter assay indicated that ATF4 knockdown significantly decreased luciferase activity in 293T and MC3T3-E1 cells transfected with the FSP1-WT luciferase reporter vector, whereas it had minimal effects on cells transfected with FSP1-Mut luciferase vectors (Fig. 2F). We overexpressed ATF4 and knocked down FSP1 in HG-treated MC3T3-E1 cells to determine the role of ATF4 in FSP1-regulated ferroptosis in osteoporosis. ATF4 overexpression reversed the inhibitory effect of FSP1 depletion on FSP1 expression in MC3T3-E1 cells treated with or without HG (Fig. 2G, H). Furthermore, HG caused elevated levels of lipid peroxidation and cellular Fe^{2+}, and ATF4 overexpression rescued the FSP1-depletion-induced increase in Fe^{2+} and lipid ROS levels in HG-treated MC3T3-E1 cells (Fig. 2I, J), indicating that ATF4 inhibits ferroptosis via FSP1.

YBX1 knockdown in MC3T3-E1 cells induced ferroptosis

Given the role of ATF4 in ferroptosis in MC3T3-E1 cells, we predicted that ATF4 is a target gene of YBX1 using the Rm2Target database. We then investigated the role of YBX1 in ferroptosis. The expression of YBX1 decreased in D-gal-treated MC3T3-E1 cells and remained unchanged after Fer-1 treatment (Fig. 3A). We successful constructed YBX1 knockdown MC3T3-E1 cells and validated shYBX1 transfection efficiency (Fig. 3B). Moreover, depletion of YBX1 aggravated the decrease in YBX1 levels in HG-induced MC3T3-E1 cells, indicating that YBX1 knockdown was effective in the in vitro osteoporosis model (Fig. 3C). Furthermore, HG elevated the levels of lipid ROS and cellular Fe^{2+}, and this effect was intensified after YBX1 knockdown (Fig. 3D, E), indicating that YBX1 inhibits ferroptosis.

YBX1 increased ATF4 mRNA stability in an m5C-dependent manner in MC3T3-E1 cells

YBX1 is an m^5C "reader" enzyme that regulates mRNA stability by recognizing m^5C modifications [21]. To determine the interaction between YBX1 and ATF4 mRNA, RNA pull-down assays were performed to explore targets of ATF4 mRNA, and YBX1 could be pulled down by ATF4 mRNA, but the antisense ATF4 mRNA (As-ATF4) used as a negative control did not pulled YBX1 down (Fig. 4A). Moreover, RIP assays showed increased enrichment of ATF4 mRNA in the complex immunoprecipitated by the YBX1 antibody, confirming the direct interaction between YBX1 and ATF4 mRNA (Fig. 4B). Subsequently, we constructed ATF4 mutants with mutations at the m^5C locus. The results showed that knockdown of YBX1 did not affect the luciferase activity of ATF4-Mut but significantly reduced the luciferase activity of ATF4-WT in 293T and MC3T3-E1 cells. This indicates that YBX1 binds to the m^5C locus of ATF4 mRNA, demonstrating that YBX1 regulates ATF4 mRNA in an m^5C-dependent manner (Fig. 4C). To confirm the regulatory effect of YBX1 on ferroptosis in osteoporosis, YBX1 was knocked down in MC3T3-E1 cells by transfection with shYBX1, and the protein level of ATF4 was significantly reduced after shYBX1 transfection (Fig. 4D). Finally, the remaining ATF4 mRNA levels decreased over time following YBX1 knockdown after the addition of actinomycin D (Fig. 4E). These results demonstrate that YBX1 regulates ATF4 stability by binding to m^5C-modified ATF4 mRNA.

YBX1 inhibited ferroptosis through the ATF4/FSP1 axis in MC3T3-E1 cells

To further clarify the regulatory relation among YBX1, ATF4, and FSP1, we performed YBX1 knockdown and/or ATF4 overexpression in MC3T3-E1 cells and examined their protein expression levels. YBX1 knockdown reduced the expression of both ATF4 and FSP1, which was reversed by ATF4 overexpression (Fig. 5A). During HG treatment, the expression of YBX1, ATF4, and FSP1 decreased, which was exacerbated by YBX1 knockdown and reversed by ATF4 overexpression (Fig. 5B). Consistently, HG induced increased levels of lipid ROS and cellular Fe^{2+}, and this effect was further enhanced after YBX1 knockdown, which was alleviated by ATF4 overexpression (Fig. 5C, D). These results indicate that YBX1 inhibits ferroptosis through the ATF4/FSP1 axis.

Discussion

More than 200 million people worldwide have osteoporosis. In addition to the physical and psychological damage to individuals, the public health burden is even greater. In the United States, the economic impact of osteoporosis on the healthcare system is projected to

reach $25.3 billion per year by 2025. This situation is exacerbated by an aging population. Therefore, studying the different signaling pathways involved in osteoporosis and their crosstalk is essential for a complete understanding of its pathogenesis and for the development of new, nontoxic, and effective treatments. Recent studies have identified ferroptosis as an independent risk factor for osteoporosis, making it a new target for interventions. It has been shown that ferroptosis can cause an imbalance between osteoblasts and osteoclasts by regulating cellular glycolipotoxicity, leading to bone loss, bone remodeling, and, ultimately, osteoporosis [22]. In this study, we used MC3T3-E1 cells to induce osteoporosis in vitro and investigated the specific mechanisms of ferroptosis in osteoblasts.

FSP1 is a key negative regulator of ferroptosis that plays a protective role in many diseases, such as attenuating white matter damage after brain hemorrhage, rescuing neuronal death, and preventing toxic damage to the liver and kidneys [23]. In bone diseases, FSP1 has been found to cause bone loss by mediating ferroptosis in macrophages [11]. FSP1 also serves as a marker for predicting ferroptosis in osteosarcoma and is a potential therapeutic target. Our results show that FSP1 knockdown consistently promoted ferroptosis in D-gal-induced osteogenic precursor cells (MC3T3-E1). ATF4 is a member of the basic leucine zipper transcription factor family that regulates the transcription of ferroptosis-related genes and acts through different pathological processes, such as hepatorenal toxic injury, neuronal cell death, and angiogenesis [24]. ATF4 binds to the TRB3 promoter, mediates oxidative stress, binds to serine pathway genes, regulates amino acid metabolism, binds to the osteocalcin promoter, and promotes osteoblast differentiation [25]. We found that ATF4 binds to the FSP1 promoter, further inhibiting ferroptosis in MC3T3-E1 cells. Overexpression of ATF4 reversed the promotion of ferroptosis caused by FSP1 knockdown, suggesting that ATF4 exerts its anti-osteoporotic effects partly by modulating downstream FSP1. In addition, ATF4 is involved in inhibiting osteoporosis by regulating osteoblast and osteoclast homeostasis and participating in osteoblast dysfunction caused by endoplasmic reticulum stress [26]. ATF4 primarily binds to the FSP1 promoter; therefore, its site of action is intracellular. Fer-1 is a lipid ROS scavenger with an N-cyclohexyl portion that acts as a lipophilic anchor within biological membranes, functioning downstream of FSP1. Therefore, Fer-1 treatment did not recover HG-reduced FSP1, ATF4, and YBX1 levels. In conclusion, ATF4 binds to the FSP1 promoter to regulate ferroptosis in osteoblasts.

YBX1 plays a role in an m^5C-dependent manner and inhibits upstream ferroptosis by regulating the ATF4/FSP1 axis in osteoblasts. Acting as a "reader" of m^5C, YBX1 is an RNA-binding protein that binds to RNA and regulates RNA stability, splicing, modification, translation, and localization, thereby increasing RNA stability [21, 27]. There are few studies on the involvement of YBX1 in the process of ferroptosis in bone diseases, and our study found that knockdown of YBX1 resulted in ferroptosis in osteoblasts. In bone formation, YBX1 can activate TGF-β signaling after binding to promoter regions, which promotes the proliferation and osteogenic differentiation of bone marrow mesenchymal stem cells [28]. YBX1 also maintains the correct splicing of genes associated with osteogenic differentiation and senescence in bone marrow stromal cells, contributing to the dynamic balance between bone loss and bone formation [29]. In addition, both RNA pulldown and RIP experiments suggested mutual binding between YBX1 and ATF4 mRNA, and the dual-luciferase assay revealed that YBX1 could bind to ATF4 mRNA in an m^5C-dependent manner.

We also found that YBX1 increased the stability of ATF4 mRNA in osteoblasts, consistent with studies showing that YBX1 maintains stability by regulating mRNA splicing and decay. For example, YBX1 recognizes m^5C modifications to maintain CHD3 mRNA stability [30]. Finally, we investigated the relations among YBX1, ATF4, and FSP1 expression. Our findings indicate that YBX1 inhibits ferroptosis in MC3T3-E1 cells via the ATF4/FSP1 axis by recognizing the m^5C modification of ATF4 mRNA. This is the first study to clarify the YBX1-mediated changes during ferroptosis, providing insights into potential therapeutic targets for the treatment of osteoporosis.

Collectively, our study demonstrated the regulatory mechanism of ferroptosis in osteoporotic lesions: YBX1 inhibited osteoblast ferroptosis in an m^5C-dependent manner via the ATF4/FSP1 axis, with ATF4 acting by binding to the FSP1 promoter. This provides novel insights into the development of osteoporosis and a theoretical basis for new treatments. However, as this study involved only in vitro experiments, strong in vivo evidence is still lacking, and future validation of these findings in animal models is needed. In addition, the direct binding of ATF4 to the FSP1 promoter to drive the inhibition of ferroptosis is not yet fully clear, and further experiments are required to verify this.

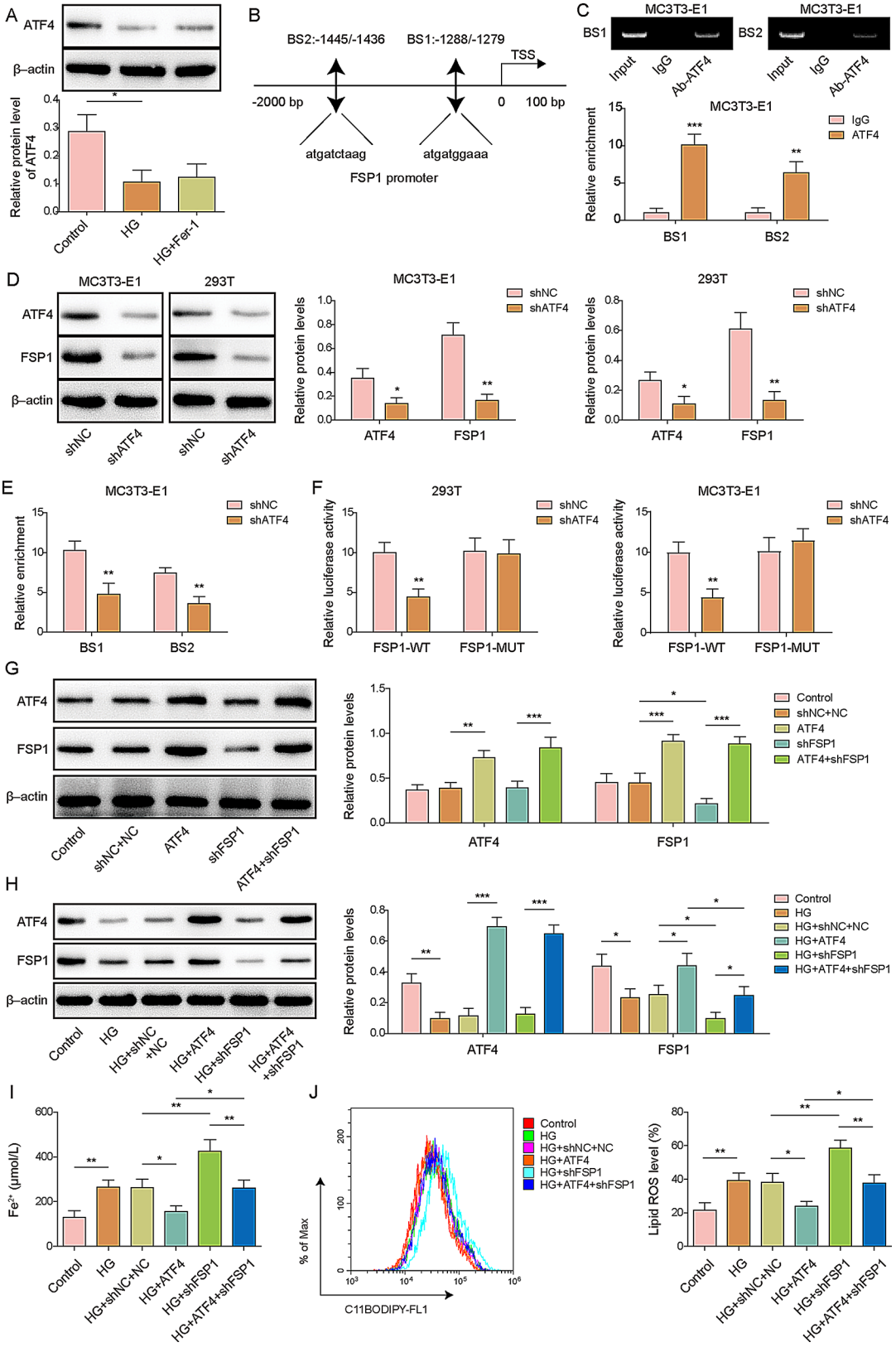

Fig. 2 (See legend on next page.)

(See figure on previous page.)

Fig. 2 Effect of ATF4 binding to FSP1 promoters in MC3T3-E1 cells on ferroptosis. MC3T3-E1 cells were used to construct an in vitro osteoporosis model by treating them with D-galactose (25.5 mM) or without (control). The cells were then treated with Ferrostatin-1 (Fer-1). (**A**) ATF4 protein expression and quantification in MC3T3-E1 cells with and without Fer-1 treatment were assessed. (**B**) JASPAR prediction of ATF4 binding to the FSP1 promoter. (**C**) A ChIP assay confirmed the interaction between ATF4 and the FSP1 promoter in MC3T3-E1 cells. (**D**) ATF4 and FSP1 protein expression and quantification in shATF4- and shNC-transfected MC3T3-E1 and 293T cells were measured. (**E**) ChIP analysis of the interaction between ATF4 and the FSP1 promoter in shATF4- or shNC-transfected MC3T3-E1 cells. (**F**) Relative luciferase activity in ATF4-knockdown 293T and MC3T3-E1 cells transfected with either FSP1-WT or FSP1-Mut. (**G**) Quantification of ATF4 and FSP1 protein expression levels in MC3T3-E1 cells transfected with shFSP1 or ATF4 overexpression vectors, shFSP1 plus ATF4 overexpression vectors, or shNC plus NC. (**H**) ATF4 and FSP1 protein expression levels and quantification in high-glucose (HG)-treated MC3T3-E1 cells transfected with shFSP1 or ATF4 overexpression vectors, shFSP1 plus ATF4 overexpression vectors, or shNC plus NC. (**I**) Cellular Fe^{2+} concentrations in HG-treated MC3T3-E1 cells transfected with shFSP1 or ATF4 overexpressing vectors, shFSP1 plus ATF4 overexpressing vectors, or shNC plus NC. (**J**) Lipid ROS levels in HG-treated MC3T3-E1 cells transfected with shFSP1 or ATF4 overexpression vectors, shFSP1 plus ATF4 overexpression vectors, or shNC plus NC. TSS: Transcription Start Site. Input: positive control. WT: wild type. Mut: mutant. $n = 3$. Data are shown as mean ± SD. * $P < 0.05$, ** $P < 0.01$, and *** $P < 0.001$. FSP1, Ferroptosis suppressor protein 1; ROS, reactive oxygen species; ATF4, activating transcription factor 4; ChIP, chromatin immunoprecipitation

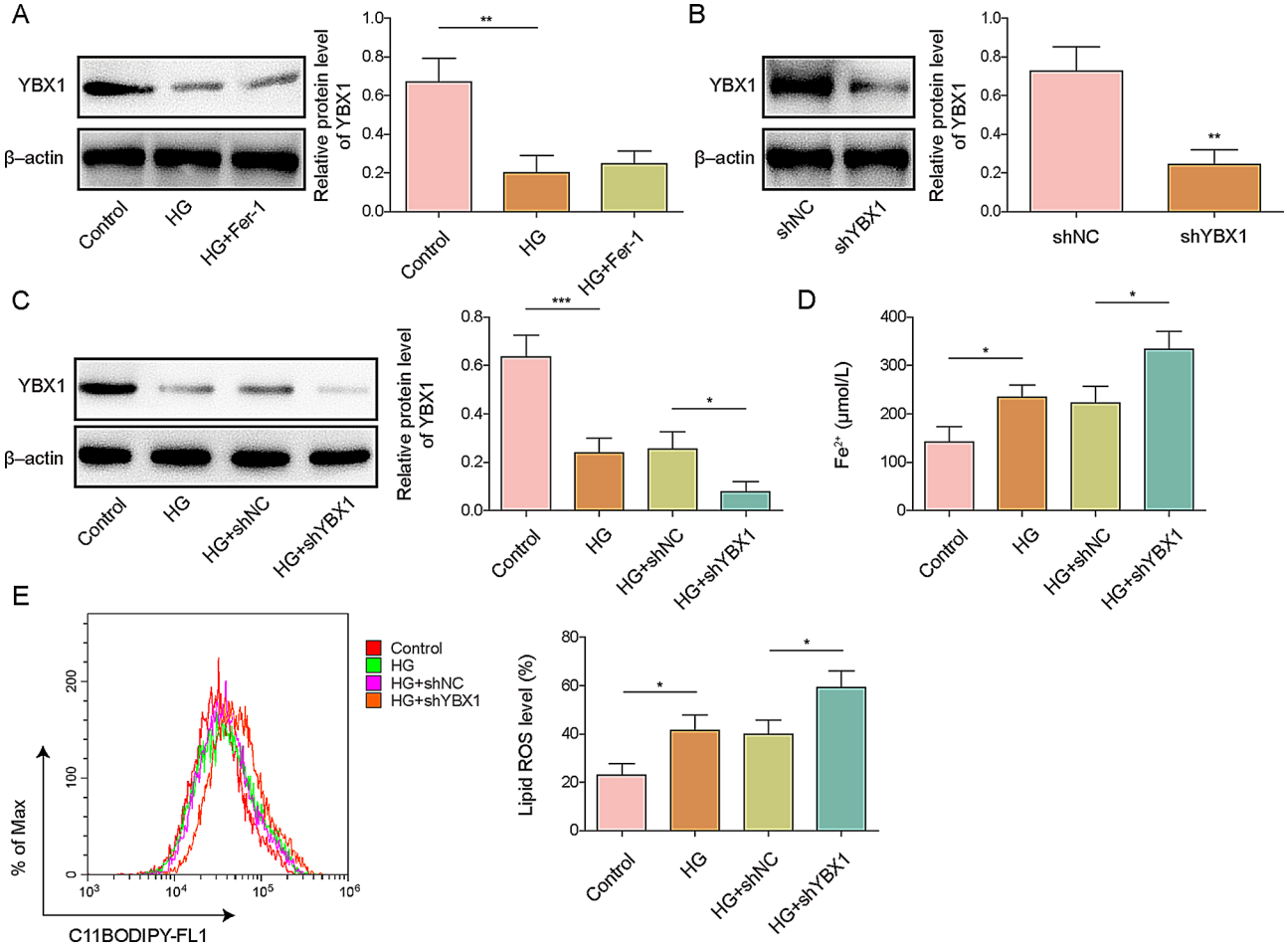

Fig. 3 Effect of YBX1 in MC3T3-E1 cells on ferroptosis. MC3T3-E1 cells were used to construct an in vitro osteoporosis model by treating them with D-galactose (25.5 mM) or without (control). The cells were additionally treated with Ferrostatin-1 (Fer-1). (**A**) YBX1 protein expression levels and quantification in high-glucose (HG)-treated MC3T3-E1 cells with or without Fer-1 treatment were assessed. (**B**) YBX1 protein expression levels and quantification in shYBX1- or shNC-transfected MC3T3-E1 cells. (**C**) YBX1 protein expression and quantification in shYBX1- and shNC-transfected HG-induced MC3T3-E1 cells. (**D**) Cellular Fe^{2+} concentrations in shYBX1- or shNC-transfected HG-induced MC3T3-E1 cells. (**E**) Lipid ROS levels in shYBX1- and shNC-transfected HG-induced MC3T3-E1 cells. $n = 3$. Data are shown as mean ± SD. * $P < 0.05$, ** $P < 0.01$, and *** $P < 0.001$. ROS, reactive oxygen species; YBX1, Y-box binding protein 1

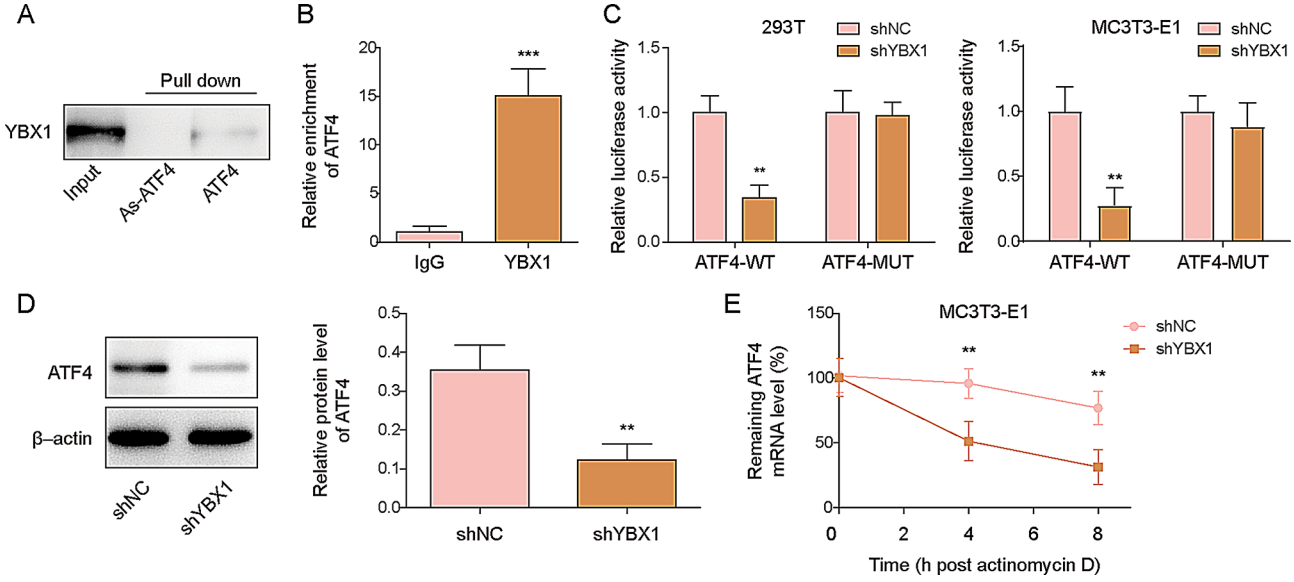

Fig. 4 Effect of YBX1 in MC3T3-E1 cells on ATF4 mRNA stability. (**A**) RNA pulldown indicated YBX1 protein binding to ATF4 mRNA. (**B**) RIP demonstrated YBX1 protein binding to ATF4 mRNA. (**C**) Relative luciferase activity in YBX1 knockdown 293T and MC3T3-E1 cells transfected with ATF4-WT or ATF4-Mut. (**D**) ATF4 protein expression levels and quantification in shYBX1- or shNC-transfected MC3T3-E1 cells. (**E**) RT-qPCR evaluated the degradation of ATF4 mRNA after treatment with actinomycin D. Input: positive control. WT: wild type. Mut: mutant. As: antisense strand. $n = 3$. Data are shown as mean ± SD. * $P < 0.05$, ** $P < 0.01$, and *** $P < 0.001$. YBX1, Y-box binding protein 1; ATF4, activating transcription factor 4; RT-qPCR, quantitative real-time polymerase chain reaction; RIP, RNA immunoprecipitation

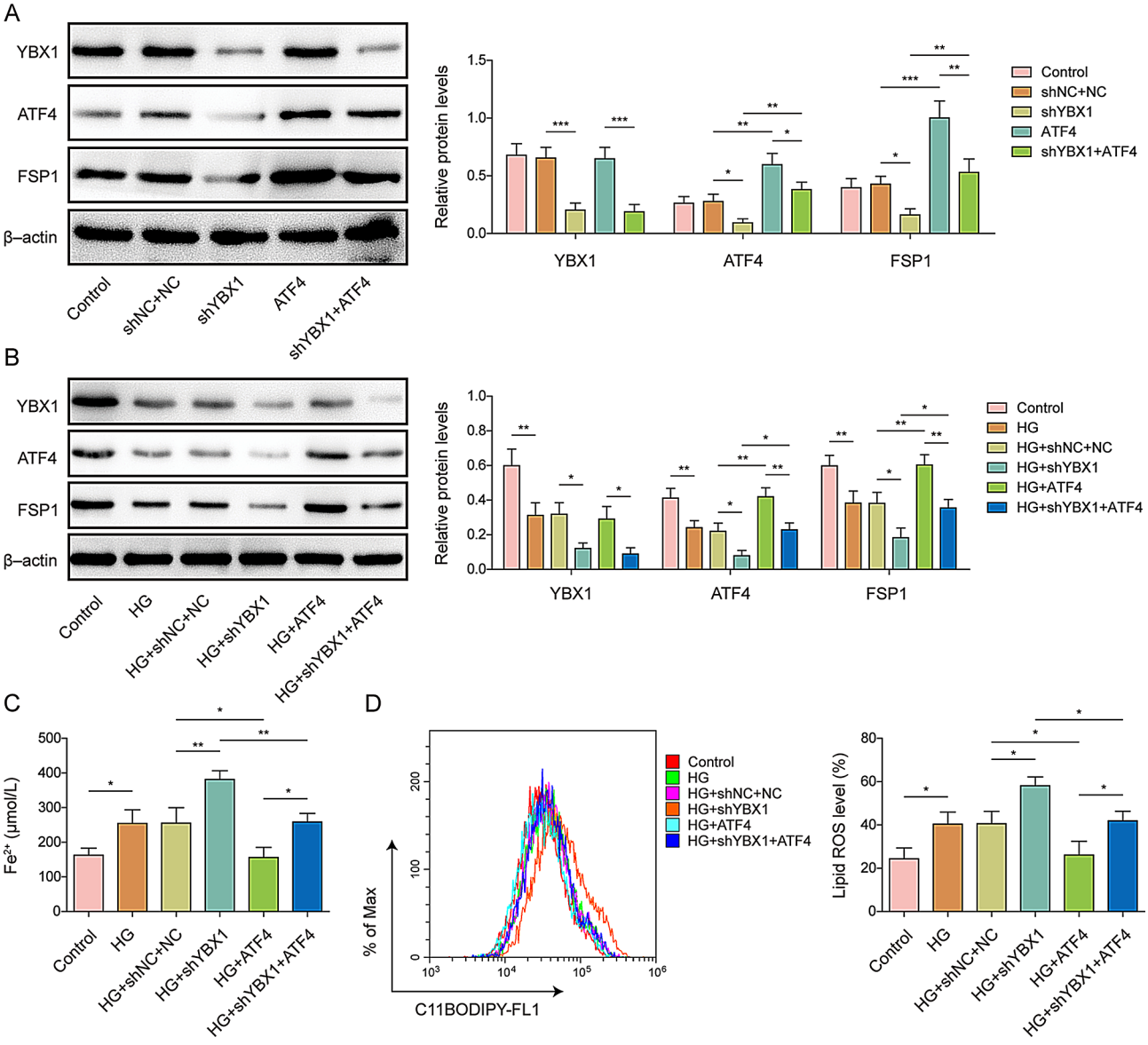

Fig. 5 Effect of YBX1 in MC3T3-E1 cells on ferroptosis through the ATF4/FSP1 axis. (**A**) YBX1, ATF4, and FSP1 protein expression levels in MC3T3-E1 cells transfected with shYBX1 or ATF4 overexpression vectors, shYBX1 plus ATF4 overexpression vectors, or shNC plus NC. (**B**) YBX1, ATF4, and FSP1 protein expression levels and quantification in high-glucose (HG)-treated MC3T3-E1 cells transfected with shYBX1 or ATF4 overexpression vectors, shYBX1 plus ATF4 overexpression vectors, or shNC plus NC. (**C**) Cellular Fe^{2+} concentrations in HG-treated MC3T3-E1 cells transfected with shYBX1 or ATF4 overexpression vectors, shYBX1 plus ATF4 overexpression vectors, or shNC plus NC. (**D**) Lipid ROS levels in HG-treated MC3T3-E1 cells transfected with shYBX1 or ATF4 overexpression vectors, shYBX1 plus ATF4 overexpression vectors, or shNC plus NC. $n = 3$. Data are shown as mean ± SD. * $P < 0.05$, ** $P < 0.01$, and *** $P < 0.001$. YBX1, Y-box binding protein 1; ATF4, activating transcription factor 4; FSP1, Ferroptosis suppressor protein 1; ROS, reactive oxygen species

Abbreviations

FSP1	Ferroptosis suppressor protein 1
AIMF2	Apoptosis-inducing factor mitochondria-associated 2
ATF4	Activating transcription factor
YBX1	Y-box binding protein 1
m^5C	5-methylcytosine
D-gal	D-galactose
ROS	Reactive oxygen species

Supplementary Information

The online version contains supplementary material available at https://doi.org/10.1186/s13018-024-05119-7.

Supplementary Material 1

Author contributions

Lei Tong: Conceptualization; Resources; Writing - Original Draft; Methodology; Formal analysis; Yanbo Chen: Validation; Investigation; Yan Gao: Data Curation; Visualization; Xiaoming Gao: Supervision; Project administration; Yanming Hao: Writing - Review & Editing; Funding acquisition.

Funding

Study on Kunshan First People's Hospital Medical and Health Science and Technology Innovation Special Project (No.KETDCX202415) and the mechanism of H2S-mediated CD31 regulation of bone H-type vessels in osteoporosis (KS2312).

Data availability

Data sharing is not applicable to this article as no new data were created or analyzed in this study.

Declarations

Ethics approval

N/A.

Competing interests

The authors declare no competing interests.

Author details

[1]Kunshan First People's Hospital Joint Surgery Department, 566 Qianjin East Road, Kunshan City, Suzhou, Jiangsu Province 215399, China

Received: 9 August 2024 / Accepted: 26 September 2024
Published online: 04 January 2025

References

1. Migliorini F, Giorgino R, Hildebrand F, et al. Fragility fractures: risk factors and management in the elderly. J. 2021;57:1119.
2. Migliorini F, Maffulli N, Colarossi G, et al. Effect of drugs on bone mineral density in postmenopausal osteoporosis: a bayesian network meta-analysis. [J]. 2021;16:533.
3. Migliorini F, Colarossi G, Baroncini A, et al. Pharmacological management of postmenopausal osteoporosis: a level I evidence based-expert opinion. J. 2021;14:105–19.
4. Migliorini F, Maffulli N, Spiezia F, et al. Biomarkers as therapy monitoring for postmenopausal osteoporosis: a systematic review. [J]. 2021;16:318.
5. Migliorini F, Maffulli N, Spiezia F, et al. Potential of biomarkers during pharmacological therapy setting for postmenopausal osteoporosis: a systematic review. [J]. 2021;16:1–13.
6. Migliorini F, Colarossi G, Eschweiler J, et al. Antiresorptive treatments for corticosteroid-induced osteoporosis: a bayesian network meta-analysis. [J]. 2022;143:46–56.
7. Conti V, Russomanno G, Corbi G, et al. A polymorphism at the translation start site of the vitamin D receptor gene is associated with the response to anti-osteoporotic therapy in postmenopausal women from southern Italy. [J]. 2015;16:5452–66.
8. Qaseem A, Forciea MA, McLean RM et al. Treatment of Low Bone Density or Osteoporosis to Prevent Fractures in Men and Women: A Clinical Practice Guideline Update From the American College of Physicians, [J]. Ann Intern Med, 166 (2017) 818-839.10.7326/M15-1361.
9. Cao Z, Xue Y, Wang J. Screening diagnostic markers of osteoporosis based on ferroptosis of osteoblast and osteoclast, [J]. Aging (Albany NY), 15 (2023) 9391-9407.10.18632/aging.204945.
10. Doll S, Freitas FP, Shah R, et al. FSP1 is a glutathione-independent ferroptosis suppressor. J. 2019;575:693–8. https://doi.org/10.1038/s41586-019-1707-0.
11. Yang M, Shen Z, Zhang X et al. Ferroptosis of macrophages facilitates bone loss in apical periodontitis via NRF2/FSP1/ROS pathway, [J]. Free Radic Biol Med, 208 (2023) 334-347.10.1016/j.freeradbiomed.2023.08.020.
12. Yuan F, Zhou Z, Wu S et al. Intestinal activating transcription factor 4 regulates stress-related behavioral alterations via paraventricular thalamus in male mice, [J]. Proc Natl Acad Sci U S A, 120 (2023) e2215590120.10.1073/pnas.2215590120.
13. Xiao Y, Xie X, Chen Z et al. Advances in the roles of ATF4 in osteoporosis, [J]. Biomed Pharmacother, 169 (2023) 115864.10.1016/j.biopha.2023.115864.
14. Jayaram N, Usvyat D. A.C.J.B.b. R. Martin, evaluating tools for transcription factor binding site prediction. [J]. 2016;17:1–12.
15. Liu WW, Zheng SQ, Li T et al. RNA modifications in cellular metabolism: implications for metabolism-targeted therapy and immunotherapy, [J]. Signal Transduct Target Ther, 9 (2024) 70.10.1038/s41392-024-01777-5.
16. Yang C, Dong Z, Ling Z, et al. The crucial mechanism and therapeutic implication of RNA methylation in bone pathophysiology. J. 2022;79:101641. https://doi.org/10.1016/j.arr.2022.101641.
17. Chetty VK, Ghanam J, Lichá K, et al. Y-box binding protein 1 in small extracellular vesicles reduces mesenchymal stem cell differentiation to osteoblasts—implications for acute myeloid leukaemia. J. 2024;13:e12417. https://doi.org/10.1002/jev2.12417.
18. Jerebtsova M, Kumari N, Xu M, et al. HIV-1 resistant CDK2-knockdown macrophage-like cells generated from 293T cell-derived human induced pluripotent stem cells. J. 2012;1:175–95.
19. Xu P, Lin B, Deng X et al. VDR activation attenuates osteoblastic ferroptosis and senescence by stimulating the Nrf2/GPX4 pathway in age-related osteoporosis, [J]. Free Radic Biol Med, 193 (2022) 720-735.10.1016/j.freeradbiomed.2022.11.013.
20. Yang WS. B.R.J.T.i.c.b. Stockwell, Ferroptosis: death by lipid peroxidation, [J]. 26 (2016) 165-176.10.1016/j.tcb.2015.10.014.
21. Liu L, Chen Y, Zhang T et al. YBX1 Promotes Esophageal Squamous Cell Carcinoma Progression via m5C-Dependent SMOX mRNA Stabilization, [J]. (2024) 2302379.10.1002/advs.202302379.
22. Yin Y, Chen GJ, Yang C et al. Osteocyte ferroptosis induced by ATF3/TFR1 contributes to cortical bone loss during ageing, [J]. Cell Prolif, (2024) e13657.10.1111/cpr.13657.
23. Wang B, Zhang X, Zhong J et al. Dexpramipexole Attenuates White Matter Injury to Facilitate Locomotion and Motor Coordination Recovery via Reducing Ferroptosis after Intracerebral Hemorrhage, [J]. Oxid Med Cell Longev, 2022 (2022) 6160701.10.1155/2022/6160701.
24. Jiang H, Wang C, Zhang A et al. ATF4 protects against sorafenib-induced cardiotoxicity by suppressing ferroptosis, [J]. Biomed Pharmacother, 153 (2022) 113280.10.1016/j.biopha.2022.113280.
25. Zhao E, Ding J, Xia Y et al. KDM4C and ATF4 Cooperate in Transcriptional Control of Amino Acid Metabolism, [J]. Cell Rep, 14 (2016) 506-519.10.1016/j.celrep.2015.12.053.
26. Su S, Zhang D, Liu J et al. Folate ameliorates homocysteine-induced osteoblast dysfunction by reducing endoplasmic reticulum stress-activated PERK/ATF-4/CHOP pathway in MC3T3-E1 cells, [J]. J Bone Miner Metab, 40 (2022) 422-433.10.1007/s00774-022-01313-x.
27. Liu X, Wei Q, Yang C, et al. RNA m5C modification upregulates E2F1 expression in a manner dependent on YBX1 phase separation and promotes tumor progression in ovarian cancer. J. 2024;1–16. https://doi.org/10.1038/s12276-024-01184-4.
28. Li B, Wang J, Xu F et al. LncRNA RAD51-AS1 Regulates Human Bone Marrow Mesenchymal Stem Cells via Interaction with YBX1 to Ameliorate Osteoporosis, [J]. Stem Cell Rev Rep, 19 (2023) 170-187.10.1007/s12015-022-10408-x.
29. Xiao Y, Cai GP, Feng X et al. Splicing factor YBX1 regulates bone marrow stromal cell fate during aging, [J]. EMBO J, 42 (2023) e111762.10.15252/embj.2022111762.

30. Meng H, Miao H, Zhang Y et al. YBX1 promotes homologous recombination and resistance to platinum-induced stress in ovarian cancer by recognizing m5C modification, [J]. (2024) 217064.10.1016/j.canlet.2024.217064.